Journal of
Medicinal Chemistry

Article

“A Sweet Combination”: Developing saccharin and acesulfame K structures for selectively targeting the tumor-associated carbonic anhydrases IX and XII.

Silvia Bua, Carrie L. Lomelino, Akilah B. Murray, Sameh M. Osman, Zeid Abdullah Alothman, Murat Bozdag, Hatem A. Abdel Aziz, Wagdy M. Eldehna, Robert McKenna, Alessio Nocentini, and Claudiu Trandafir Supuran

J. Med. Chem., **Just Accepted Manuscript** • DOI: 10.1021/acs.jmedchem.9b01669 • Publication Date (Web): 03 Dec 2019

Just Accepted

is published by the American Chemical Society. 1155 Sixteenth Street N.W., Washington, DC 20036

"A Sweet Combination": Developing saccharin and acesulfame K structures for selectively targeting the tumor-associated carbonic anhydrases IX and XII.

Silvia Bua[a], Carrie Lomelino[b], Akilah B. Murray[b], Sameh M. Osman[c], Zeid A. ALOthman[c], Murat Bozdag[a], Hatem A. Abdel-Aziz[d], Wagdy M. Eldehna[e], Robert McKenna[b], Alessio Nocentini[a,*], Claudiu T. Supuran[a,*].

[a]*University of Florence, Department of NEUROFARBA, Section of Pharmaceutical and Nutraceutical Sciences, via Ugo Schiff 6, 50019, Sesto Fiorentino, Florence, Italy*

[b]*University of Florida, Department of Biochemistry and Molecular Biology, 1200 Newell Dr, Gainesville, FL 32610, U.S.A.*

[c]*Chemistry Department, College of Science, King Saud University, P. O. Box 2455, Riyadh 11451, Saudi Arabia.*

[d]*Department of Applied Organic Chemistry, National Research Center, Dokki, Giza, P.O. Box 12622, Egypt*

[e]*Department of Pharmaceutical Chemistry, Faculty of Pharmacy, Kafrelsheikh University, Kafrelsheikh 33516, Egypt*

ABSTRACT

The sweeteners saccharin (**SAC**) and acesulfame K (**ACE**) recently entered the topic of anticancer human carbonic anhydrase (CA, EC 4.2.1.1) inhibitors as they showed to selectively inhibit the tumor-associated CAs IX/XII over ubiquitous CAs. A drug design strategy is here reported which took **SAC** and **ACE** as leads and produced a series of 2H-benzo[e][1,2,4]thiadiazin-3(4H)-one-1,1-dioxides (**BTD**). Many derivatives showed greater potency (K_Is-CA IX 19.1-408.5 nM) and selectivity (II/IX *SI* 2-76) than the leads (K_Is-CA IX 103, 2400 nM; II/IX-*SI* 56, >4) against CA IX/XII over off-target isoforms. A thorough X-ray crystallographic study depicted their binding mode to both CA II and IX-mimic. The most representative **BTDs** were characterized *in vitro* for their antitumor activity against A549, PC-3 and HCT-116 cancer cell lines both in normoxia and hypoxia. The two most effective compounds were assayed for their effect on several apoptosis markers, identifying promising leads for the development of new anticancer drugs.

Keywords: tumor; metalloenzyme; sweetener; saccharin; acesulfame; optimization; inhibition.

1. Introduction

The tumor microenvironment considerably influences cancerogenesis.[1-3] Hypoxic tumors are often characterized by a disproportion between the demand of rapidly proliferating cancer cells and the ability of the forming vascular system to provide an adequate oxygen supply.[4,5] As a response, cancer cells adapt their metabolism by undergoing a glycolytic shift, which decreases cellular pH and changes gene expression patterns in order to survive in an environment unsuitable for normal cell growth.[4,5] Notably, an orchestra of membrane proteins, among which transporters such as sodium-proton exchangers (NHE1), anion exchangers (AE2), sodium-bicarbonate transporters (NBCe1), monocarboxylate transporters (MCT4) and carbonic anhydrases (CA, EC 4.2.1.1), is assembled to regulate the pH within and outside the cells, maintaining a slightly alkaline intracellular pH and acidifying the extracellular environment.[1-5] CA isoform IX (CA IX), which is not significantly expressed in most normal tissues, has been shown to be associated with hypoxic cancer phenotypes.[4-8] CA XII also intervenes in the microenvironment acidification for a number of tumor types.[4,9] Therefore CA IX and XII are factors driving tumor growth, invasiveness, proliferation, metastasis, and resistance to common radio- and chemotherapy, resulting in unfavourable prognoses for cancer patients.[3] As such, agents inhibiting CA IX and XII have shown to provide inhibition of the primary tumor growth, invasion and metastasis, and reduction of cancer stem cell population.[10]

The main challenge encountered in the design of anticancer CA inhibitors (CAIs) has been the lack of isoform-selectivity exhibited by the most classical inhibitory chemotypes, namely the sulfonamides and their bioisosteres.[11,12] A comparison of the 12 catalytically active human CAs shows a high homology between the active sites that complicates the design of disease-associated selective inhibitors.[13] Nonetheless, a plethora of strategies have been developed to overcome this issue, including the optimization of classical CAIs (i.e. the tail approach, which led to **SLC-0111**,

the first-in-class CAI entering clinical trials for the treatment of hypoxic tumors)[12] or the use of alternative chemotypes adopting different mechanisms of enzymatic inhibition.[11,12]

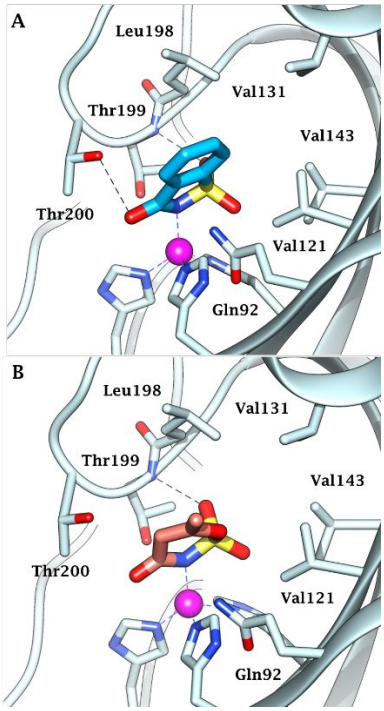

Figure 1: Active site view of the CA IX adduct with A) **SAC** (PDB 4RIV) and B) **ACE** (PDB 5WGP).

The cyclic sulfimide saccharin (**SAC**), the oldest artificial sweetener, has recently entered this topic. **SAC**, which is 450 times sweeter than sucrose, was shown to selectively discriminate among the diverse isoforms, distinctly from classical CAIs such as acetazolamide (**AAZ**).[14] It is, in particular, a selective nanomolar inhibitor of CA IX, showing weaker, micromolar inhibition of the ubiquitous CA I and II (60-fold II/IX selectivity).[14] Its cyclic acylsulfonamide, which is much more acidic than primary sulfonamides, functions as a zinc binding group (ZBG) within the CA active site. X-ray and neutron crystallography studies pointed out that alternative interactions with residue Gln67 (leading to remodelling of H-bonds and water orientations) contributed to the CA IX preferential binding of **SAC** compared to CA II (that reports an Asn in position 67).[15,16] A **SAC** derivative, called **SGC** (saccharin-glucose conjugate), was designed utilizing the tail approach with a polar carbohydrate linked by a triazole as the tail moiety of the CA inhibitor.[15] It showed even further enhanced selectivity for CA IX over both CA I and CA II (>1000-fold), with the specificity

of binding explained by evident differences in interacting active site residues between CA II and CA IX.

Another FDA approved food additive, acesulfame K (**ACE**, a cyclic acylsulfamate), was recently kinetically and structurally characterized with CAs.[17] Interestingly, **ACE** induced no inhibition of CA I, II and XII while inhibiting CA IX in the low micromolar range, with its weak inhibition being likely due to the absence of the aromatic core. Furthermore, it exhibits different active site binding modes between isoforms, namely coordinating the Zn(II) ion via the aromatic nitrogen in the case of CA IX, and anchoring to zinc-bound water molecule/hydroxide ion in CA II. This behaviour is reflected by **ACE** demonstrating measurable inhibition toward CA IX but not to other CA isoforms.[17] This study showed the value of **ACE** as a lead compound for designing new CA IX specific inhibitors.

In this context, libraries of N- and/or O-substituted **SAC** and **ACE** derivatives have been recently reported as potent and selective inhibitors of CA IX and XII.[18-20] Nonetheless, this type of functionalization decoupled these chemotypes away from a zinc-binder character (or water-anchoring, *vide supra*) promoting likely alternative binding modes, which have not yet been elucidated.

Here a new series of **SAC**- and **ACE**-based derivatives is reported by combining and developing the lead chemotypes structures to produce cyclic ureidosulfonamides, namely 2H-benzo[e][1,2,4]thiadiazin-3(4H)-one 1,1-dioxides (**BTD**), which preserve a zinc-binding group and include another foothold for ligand/target interactions and/or functionalization.

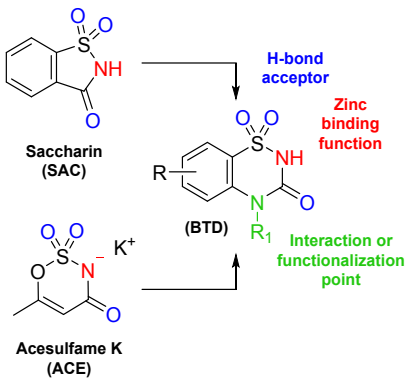

Figure 2: Rational development of benzothiadiazin-3-one 1,1-dioxides (**BTD**), based on the structures and inhibition profiles of **SAC** and **ACE**.

2. Results and discussion

2.1 Drug design and chemistry

To methodically explore the chemical space that induces cyclic acylsulfonamides or sulfamates to yield specific inhibition of CA IX and XII, an approach to merge SAC and ACE structures was developed and is here reported, producing a series of cyclic ureidosulfonamides **2a-2t**. The redesigned scaffold **BTD** preserves the zinc-binding group of SAC and ACE and includes another interaction and/or functionalization point (i.e. the NH between the carbonyl and the aromatic ring).

In order to identify new CA inhibitory chemotypes, a previous screening included the unsubstituted 2H-benzo[e][1,2,4]thiadiazin-3(4H)-one 1,1-dioxide **2a**,[21] further supporting the production of such a series as this derivative was shown to hold selectivity for CA IX/XII over CAs I and II. Here an extended SAR study was worked out by appending a wealth of substituents both in R and R_1 position (Figure 2) by exploiting a more versatile synthetic procedure than that reported by Bozdag et al. for **2a**.[21] Instead of treating *o*-aminobenzenesulfonamide with phosgene, which does not allow wide and accessible **BTD** functionalization, a forward strategy recently proposed by Zhang and Kornahrens (for providing new classes of aldose reductase and irreversible serine hydrolase inhibitors, respectively)[22,23] is here applied and extended.

The adopted synthetic procedure is depicted in *Scheme 1*. Chlorosulfonyl isocyanate (**CSI**) was treated at -40°C with commercially available variously substituted anilines (**1a-n**), N-methylanilines (**1o,p**) and indoline (**1q**) using nitromethane or nitroethane as solvent to yield the

intermediates chlorosulfamoylureas $\beta_{a\text{-}q}$. Thus, aluminium trichloride ($AlCl_3$) was added and temperature risen to 110°C to promote a Friedel-Crafts-like core cyclization. The absence of a base and a very low temperature are important to avoid reaction of the aniline with the sulfamoyl portion of **CSI**. In contrast, the choice of nitromethane or nitroethane is driven by the necessity to use a polar aprotic solvent which can span from markedly under-zero temperatures to over 100°C without solidifying or boiling. Reaction attempts with markedly electron-poor anilines of the nitro-, sulfonamido- or polyhalo-substituted types crashed with their low reactivity in both reaction steps.

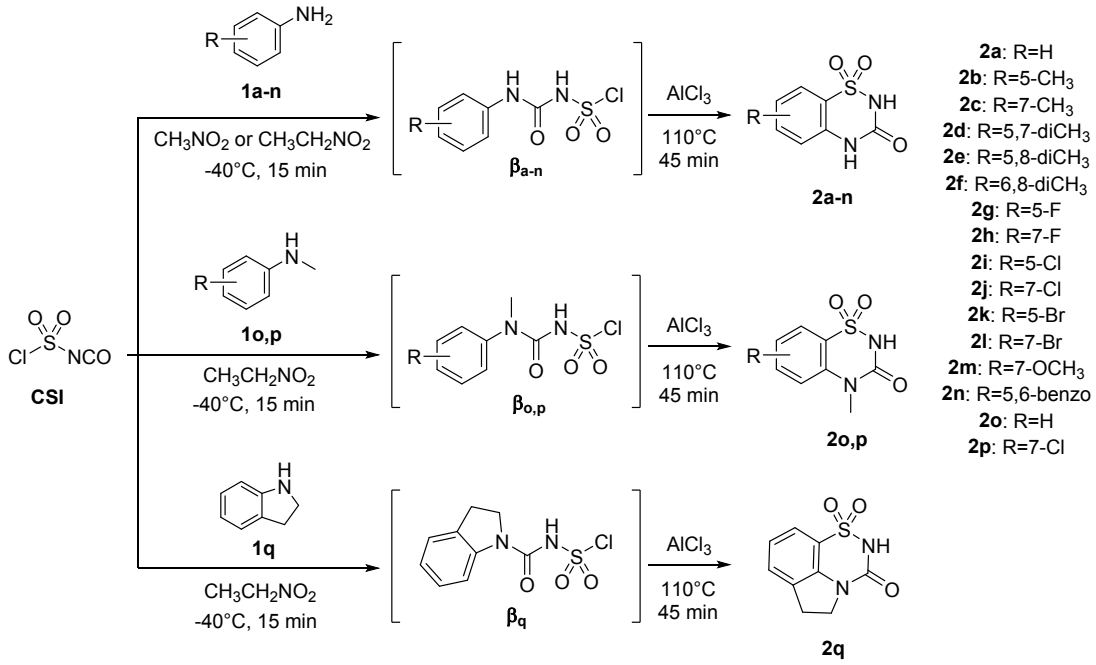

Scheme 1: Synthesis of 2H-benzo[e][1,2,4]thiadiazin-3(4H)-one 1,1-dioxides **2a-q**.

The 5- and 7-methyl derivatives **2b** and **2c** were also oxidized with potassium permanganate to give benzoic acids **2r** and **2s** respectively, as illustrated in *Scheme 2*. The 7-methoxy-**BTD** underwent demethylation by treatment with 1.0 M BBr_3 in DCM to produce alcohol **2t** (*Scheme 2*). Compounds **2a-2t** were obtained in high yields and characterized by means of ^{1}H-, ^{13}C-, ^{19}F-NMR spectroscopy and HRMS. Compounds used in biological assays were >95% pure, as determined by HPLC. Sodium salts thereof were in case produced by treating **BTD** derivatives with NaOH in methanol.

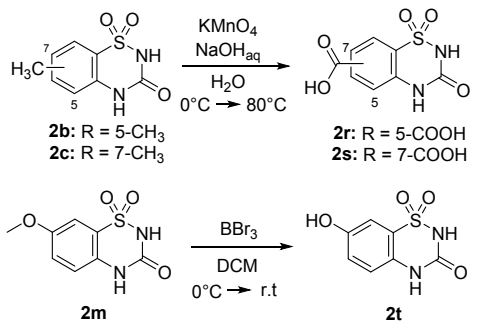

Scheme 2: Synthesis of derivatives **2r-t**.

2.2 Carbonic Anhydrases Inhibition

Compounds **2a-t** were assayed *in vitro* for their inhibitory action against six physiologically relevant human CA isoforms – i.e. the cytosolic I, II (ubiquitous isoforms) and VII (defined as a CNS-associated isozyme) and the membrane associated IV (overexpressed in some CNS tumors), IX and XII - by means of a Stopped-Flow CO_2 hydrase assay using the clinically used drug **AAZ** as a standard.[24] The following structure−activity relationship (SAR) can be assembled from the data reported in Table 1.

Table 1. Inhibition data of human CA isoforms I, II, IV, VII, IX, XII with compounds **2a-t** and the standard inhibitor acetazolamide (**AAZ**) by a Stopped Flow CO_2 Hydrase Assay.[24]

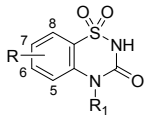

Cmpd	R	R_1	K_I (nM)[a]					
			CA I	CA II	CA IV	CA VII	CA IX	CA XII
2a[b]	H	H	866.0	150.3	675.3	465.8	78.7	53.1
2b	5-CH_3	H	968.7	143.8	1228	975.3	63.9	69.3
2c	7-CH_3	H	1066	871.7	896.6	956.0	45.8	74.3
2d	5,7-diCH_3	H	1274	763.5	1637	690.9	25.8	38.3
2e	5,8-diCH_3	H	2541	2192	1427	1899	367.6	458.7
2f	6,8-diCH_3	H	1920	2936	2692	1790	408.5	764.0
2g	5-F	H	546.7	140.1	461.0	125.5	58.4	42.7
2h	7-F	H	1289	533.6	708.6	435.5	19.1	24.9
2i	5-Cl	H	930.2	685.5	1031	389.3	28.2	42.5
2j	7-Cl	H	1864	1141	1748	1178	56.9	70.8
2k	5-Br	H	2324	526.9	853.6	620.3	73.3	75.8
2l	7-Br	H	4403	2362	1557	467.8	31.0	96.6
2m	7-OCH_3	H	3809	1922	1945	1364	35.8	64.5
2n	5,6-benzo	H	2071	483.6	2674	3949	60.2	104.9
2o	H	CH_3	3406	853.1	3459	7507	139.5	181.5
2p	7-Cl	CH_3	>10000	2337	5885	3238	188.9	325.7

2q	5-CH_2-CH_2-		6857	1060	3894	1282	273.4	247.2
2r	5-COOH	H	5783	2445	379.8	2796	91.2	27.0
2s	7-COOH	H	>10000	6775	76.1	4965	98.7	15.5
2t	7-OH	H	1894	3024	452.4	2565	88.1	34.6
SAC[c]	-		>10000	5950	7920	10	103	633
SCG[d]	-		>10000	>10000	n.d.	n.d.	50	600
ACE[e]	-		>10000	>10000	n.d.	n.d.	2400	>10000
SLC-0111	-		5080	960.0	286.0	8550	45.0	4.5
AAZ	-		250	12.5	74.0	2.5	25.0	5.7

a. Mean from 3 different assays, by a stopped flow technique (errors were in the range of ± 5-10 % of the reported values); b. data in agreement with ref. 21; c. data from ref. 14; d. data from ref. 15; e. data from ref. 17.

Most compounds among **2a-t** inhibited the ubiquitous off-target CA I in the micromolar range with inhibition constants (K_I) spanning between 1066 and over 10000 nM, whereas the unsubstituted (**2a**), 5-CH_3 (**2b**), 5-F (**2g**) and 5-Cl (**2i**) derivatives were high nanomolar inhibitors (K_Is in the range 546.7-968.7 nM).

The physiologically dominant CA II was shown to be slightly more inhibited by **BTDs** than CA I as a minor number of compounds acted in the micromolar range, from 1060 to 6775 nM (**2j**, **2l**, **2m**, **2p-t**) and most displayed medium to high nanomolar K_Is (in the range 140.1-871.7 nM). The unsubstituted (**2a**), 5-CH_3 (**2b**) and 5-F (**2g**) derivatives resulted to be the most potent CA II inhibitors of the series with K_Is of 150.3, 143.8 and 140.1 nM), showing that the CA II active site efficiently tolerates solely small substituents appended at the 5-position of the scaffold.

CA IV was inhibited in a comparable range with CA I by **BTDs 2a-2t** with most compounds functioning with K_Is between 1031 and 5885 nM, and a small subset (**2a**, **2c**, **2g**, **2h**, **2k**) acting in the high nanomolar range (461.0-896.6 nM). Of note is the case of derivatives bearing hydrophilic groups on the aromatic ring, that are **2r-t**, which showed enhanced CA IV inhibitory properties such as the 76.1 nM K_I of the 7-carboxy-**BTD 2s**. The presence of a markedly hydrophilic pocket is a unique hallmark of CA IV active site structure that might account for the inhibition data shown by **2r-t**.[25]

The other cytosolic isoform CA VII showed, in contrast, an inhibition profile that resembled that of CA II, according significant similarities existing between their active sites.[26] Nonetheless, the 5-F-**BTD 2g** solely displayed a K_I below 200 nM (125.5 nM) and the halogen swapping with a chlorine

atom produced the second best CA VII inhibitor with a K_I of 389.3 nM. Also the unsubstituted (**2a**), 7-F (**2h**) and 7-Br (**2l**) derivatives reported K_Is minor than 500 nM (435.5-467.8 nM), whereas the 5-CH_3-derivative **2b** showed a worsening of CA VII inhibition when compared to CA II (from 143.8 to 975.3 nM).

In agreement with the planned drug-design, the inhibitory profiles measured against CA IX for **BTDs 2a-2t** deviate from those of the other assayed isoforms. The compounds K_I values spanned between 19.1 and 408.5 nM. A rather flat inhibition trend can be seen from data in Table 1 for derivatives acting on CA IX below 100 nM, as K_Is lie in the range 31.0-98.7 nM, except for the 5,7-diCH_3 (**2d**), 7-F (**2h**) and 5-Cl (**2i**) derivatives which resulted to be the best CA IX inhibitor of the study with K_Is of 25.8, 19.1 and 28.2 nM, respectively. A subset of compounds, among which the 5,8-diCH_3 (**2e**) and 6,8-diCH_3 (**2f**) derivatives and the N-substituted **2o-q** reported, in contrast, over 100 nM K_Is which spanned from 139.5 and 408.5 nM.

Again, structural similarities between CA IX and XII active sites yielded analogies in the inhibitory profiles of the two isoforms with **BTDs 2a-2t**.[26] CA XII was, in fact, efficiently inhibited by most derivatives with K_Is settling in the range 15.5-764.0 nM. While the 7-F derivative **2h** retained one of the most efficient activities with a K_I of 24.9 nM, a worsening can be observed for **2d** and **2i** (K_I of 38.3 and 42.5 nM). In contrast, an inhibition increase with respect to CA IX was shown by the carboxy and hydroxy derivatives **2r-t (**K_Is in the range 15.5-34.6 nM), with the 7-carboxy **2r** resulting the best CA XII inhibitor of the series. It should be stressed that one of the dissimilarities in the active site architectures of the tumor-associated CAs is the presence of a set of Thr and Ser residues uniquely in CA XII, which might produce H-bond networks accounting for the **2r-t** inhibition potency. Again, the 5,8-diCH_3 (**2e**) and 6,8-diCH_3 (**2f**) derivatives and the N-substituted **2o-q** reported the weakest CA XII inhibition.

Overall, most compounds of the **BTD** series showed significantly improved CA IX and XII inhibitory action than the lead **SAC** (K_Is of 103 and 633 nM) and **ACE** (K_Is of 2400 and >10000

nM), but also reported an increased binding to CA I, II and IV with respect to the leads. A marked drop of efficacy was instead displayed by **2a-t** against CA VII compared to **SAC** (K_Is of 10 nM). Comparable inhibition profiles were detected for most **BTDs** with **SLC-0111**. In fact, this ureidobenzenesulfonamide, currently in Phase II/b clinical trials as antitumor CAI, inhibits CA I and VII in the low micromolar range and CA II with a K_I of 960 nM. The target CA IX is inhibited with a K_I of 45.0 nM. In contrast, it displays a more marked CA IV inhibition (K_I of 286.0 nM) than **BTD** compounds as well as a more intense inhibition of the target CA XII (K_I of 4.5 nM).

As for the selectivity of action of the newly reported CAIs, the selectivity index (*SI*) for CA IX and XII over the remaining isoforms are reported in Table S1, Supporting Information. It is noteworthy that all derivatives are selective inhibitors of the tumor-related CAs over off-target ones, with the unique exception of compound **2s** in the IV/IX ratio (*SI* = 0.8). Almost all substitution patterns on the **BTD** scaffold induced better II/IX and II/XII *SI* than the unsubstituted **2a** (1.9 and 2.8, respectively), ranging from 2.3 to 68.6 and 2.1 to 437.1, respectively. While *SI* calculated for CA VII settle in a comparable range with CA II, those reported for CA I, II and IV are markedly greater, reaching a value major than 645.2 for **2s** in the I/XII ratio.

While *SI* calculated for the clinically used **AAZ** are easily exceeded by **BTDs 2a-2t**, it is reasonable to comment on their comparison with *SI* measured for **SAC**, **SCG, ACE** and **SLC-0111**. In spite of a more efficient inhibition of off-target CAs by the **BTDs** than the leads, comparable or even more favourable *SI* could be extrapolated for many compounds of the series from the inhibition data of Table 1. In fact, depending on the substitution pattern on the main scaffold some derivatives, such as **2l**, **2m** and **2s** in the II/IX ratio and many more in the II/XII ratio, showed increased selectivity than the lead **SAC**, with the *SI* of **ACE** *SI* being difficult to comment because of its weak CA inhibition. A subset of derivatives might even compete with **SCG** in terms of I/XII and II/XII specificity of action. Finally, most **BTDs** show higher II/IX *SI* than **SLC-0111** (21.3). However, the

latter reports a rather high II/XII *SI* (213.3), which is overcome uniquely by **2s** (437.1) within the **BTD** series.

2.2 X-ray Crystallography

Crystal structures of CA II and CA IX-mimic in complex with cyclic ureidosulfonamide inhibitors **2a**, **2d**, **2h**, **2i**, and **2o** were determined in order to analyze compound binding and rationalize the observed inhibition profiles. The crystallographic data are reported in Tables S2 and S3, Supporting Information. Overall, these compounds bind similarly to the lead compounds **SAC** and **ACE** (bound in CA IX) (Figure 3).

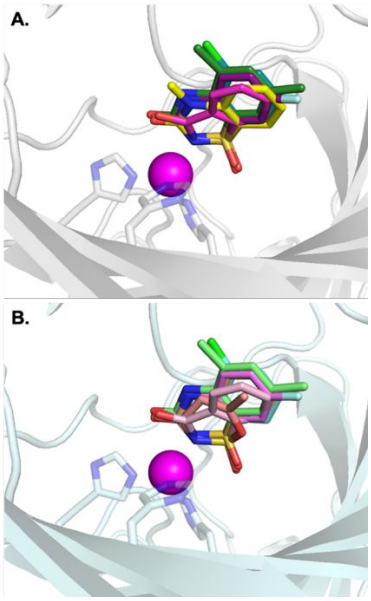

Figure 3. A) Overlay of ureidosulfonamide compounds **2a** (orange, PDB 6U4Q), **2d** (green, PDB 6UGN), **2h** (purple, PDB 6UGR), **2i** (blue, PDB 6UGP), **2o** (yellow, PDB 6UH0) and lead compound **SAC** (pink, PDB 2Q1B) in CA II. B) Overlay of ureidosulfonamide compounds **2a** (orange, PDB 6U4T), **2d** (green, PDB 6UGO), **2h** (purple, PDB 6UGZ), **2i** (blue, PDB 6UGQ) and lead compounds **SAC** (pink, PDB 4RIV) and **ACE** (salmon, PDB 5WGP) in CA IX-mimic.

As such, the aromatic N interacts directly with the zinc, displacing the zinc-bound water that is essential for catalytic activity, in addition to DW and W1 of the proton wire, which facilitate the transfer of a proton to bulk solvent during catalysis. Inhibitor binding was determined to be stabilized by the formation of hydrogen bonds between the compound carbonyl and T199 side chain hydroxyl in addition to inhibitor sulfonamide and T199 backbone amide. Binding is further

supported by VDW interactions with active site residues such as V121, F131 (CA II), V135, L141, V143, L198, T200, P202, and W209 (Figures 4 and S1, Supporting Information).

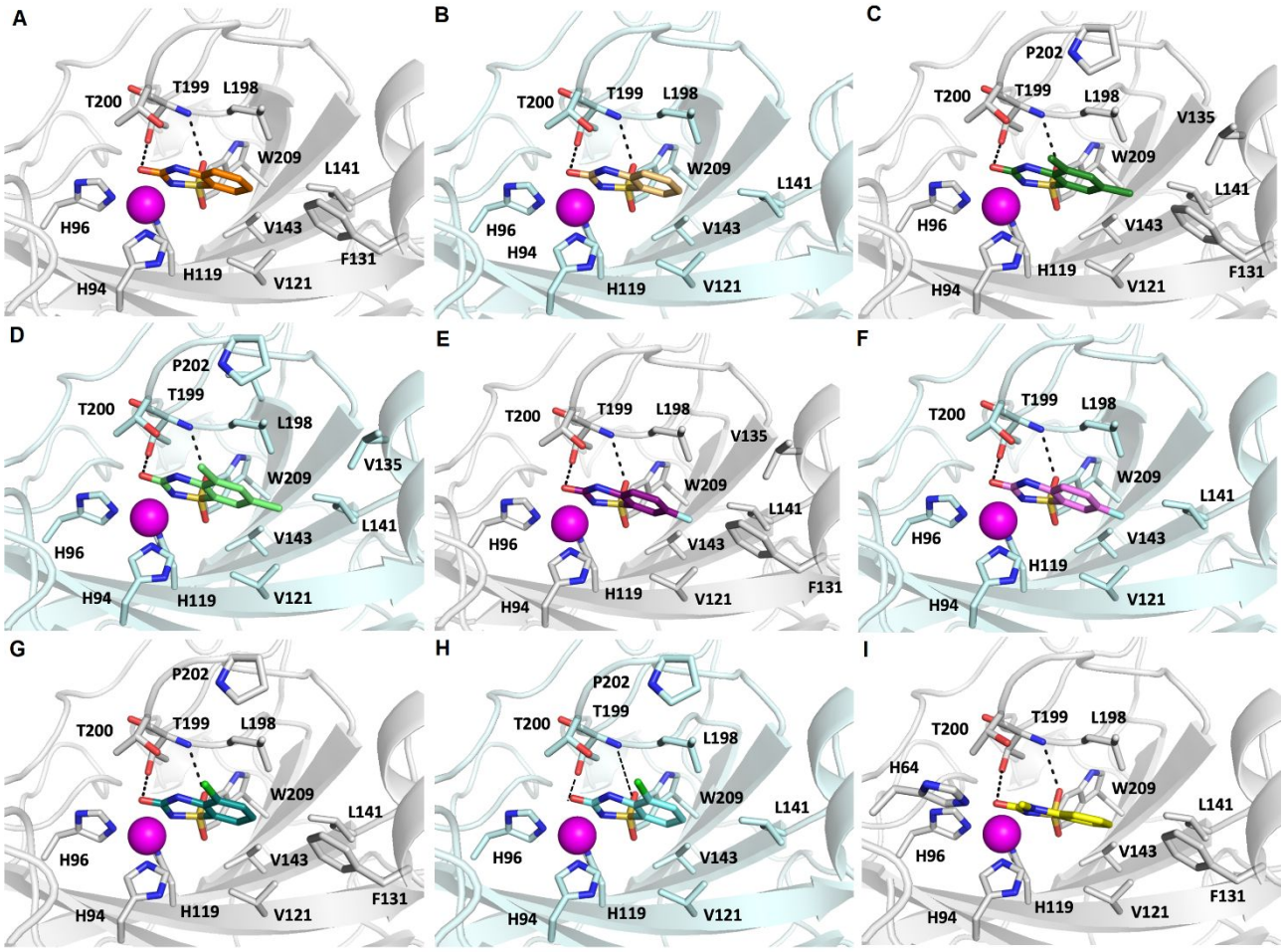

Figure 4. Binding of **BTD** compounds displayed in the active sites of CA II (gray) and CA IX-mimic (pale cyan). Hydrophobic residues are shaded orange and hydrophilic residues purple. The **2a** (panel A and B, PDBs 6U4Q and 6U4T), **2d** (panel C and D, PDBs 6UGN and 6UGO), **2h** (panel E and F, PDBs 6UGR and 6UGZ), **2i** (panel G and H, PDBs 6UGP and 6UGQ), and **2o** (panel J, PDB 6UH0) inhibitors are shown as orange, green, purple, blue, and yellow sticks, respectively.

These five compounds all exhibit a greater affinity for CA IX over the off-target, ubiquitous CA II. Interestingly, an overlay of each inhibitor bound in CA II and CA IX demonstrates that these inhibitors bind in a similar orientation in both isoforms (Figure 5) (excluding **2o** which was only determined in CA II), which has also been previously observed for **SAC** binding. Therefore, the observed specificity for CA IX is likely attributed to the feasibility of inhibitor movement and entry into the active site. CA IX has a larger hydrophobic pocket, along which substrate and many

inhibitors travel, due to residue V131 in place of F131 in CA II. The decrease in steric hindrance of this residue at the opening of the active site facilitates the binding of bulkier, aromatic compounds such as these ureidosulfonamides.

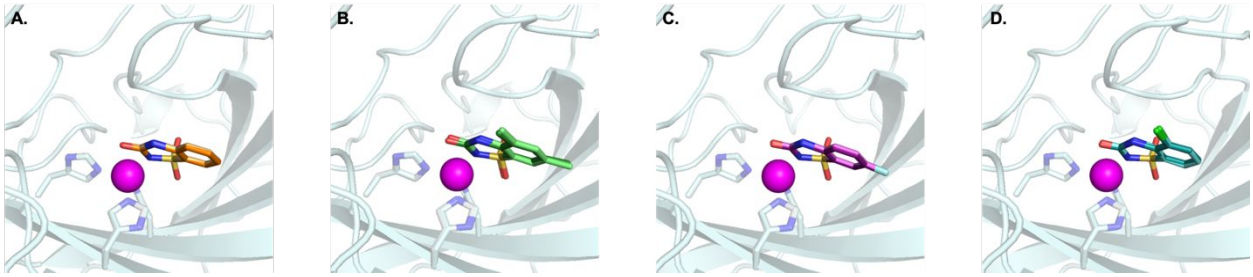

Figure 5. Overlay of inhibitors bound in CA II and CA IX-mimic. Inhibitors are displayed in the active site of CA IX-mimic as sticks. A) **2a** (orange, PDBs 6U4Q and 6U4T), B) **2d** (green, PDBs 6UGN and 6UGO), C) **2h** (purple, PDBs 6UGR and 6UGZ), and D) **2i** (blue, PDBs 6UGP and 6UGQ).

Compounds **2d**, **2h**, **2i** have similar affinities for CA IX that are approximately 3- and 7-fold higher than those of **2a** and **2o**, respectively. Generally, the affinity of the inhibitor is observed to increase with the hydrophobicity of substitutions. Substitution of two positions or the addition of a halogen increases the number and/or strength of VDW and hydrophobic interactions with surrounding active site residues. Although the structure of **2o** was not determined in complex CA IX-mimic, an overlay of the five compounds in CA II shows that **2o** is shifted, reflecting the weakest affinity observed for both CA II and CA IX. This observation can be attributed to steric hindrance of the addition methyl group on the N with the side chain of T200, likely forcing the compound to bind in a less energetically favorable orientation.

2.3 Anticancer Activity

2.3.1. Anti-proliferative activity

The *in vitro* anti-proliferative action of the **BTDs 2a**, **2d**, **2h**, **2i**, **2o** was assessed against three human cancer cell lines overexpressing CA IX, namely A549 (lung), PC-3 (prostate) and HCT-116 (colon),[27-29] using an MTT reduction assay as described by T. Mosmann.[30] Staurosporine was used as reference anticancer drug. The five **BTDs** were evaluated under both normoxic and hypoxic

conditions, where the cobalt (II) chloride hexahydrate was adopted as the chemical inducer of HIF-1α to establish the hypoxic conditions.[31] The results are expressed as IC_{50} values and listed in Table 2.

Table 2. *In vitro* anti-proliferative activity of compounds **2a**, **2d**, **2h**, **2i**, **2o** against lung A549, prostate PC-3 and colon HCT116 cancer cell lines under normoxic and hypoxic conditions.

Compound	IC_{50} (μM)[a]					
	A549		PC-3		HCT116	
	Normoxia	Hypoxia	Normoxia	Hypoxia	Normoxia	Hypoxia
2a	3.53±0.16	2.68±0.31	13.95±0.75	12.25±1.1	1.30±0.06	1.50±0.53
2d	4.77±0.22	5.74±0.28	6.31±0.41	0.82±0.06	3.85±0.22	4.18±0.27
2h	18.32±1.3	15.01±0.92	11.98±1.2	6.53±0.43	3.86±0.19	2.73±0.14
2i	10.88±0.73	7.35±0.36	16.23±0.92	3.52±0.24	5.26±0.36	7.57±0.51
2o	19.86±0.97	16.34±2.1	23.76±1.92	16.93±0.99	10.88±0.41	7.13±0.38
Staurosporine	7.47±0.39	13.22±0.82	4.91±0.17	5.92±0.24	8.86±0.33	16.15±0.57

a. IC_{50} values are the mean ± S.D. of three separate experiments.

The IC_{50} values in Table 2 revealed that **2a**, **2d**, **2h**, **2i** and **2o** exhibited moderate to excellent growth inhibition activity against the tested cancer cell lines. In particular, the assayed **BTDs** were more effective against colon HCT-116 cells than A549 and PC-3 cells, except **2d** and **2i** which displayed an enhanced growth inhibitory activity against PC-3 cells under the hypoxic conditions.

As for the activity against HCT-116, the data displayed in **Table 2** ascribed to all the examined **BTDs** excellent efficacy in inhibiting the growth of the cells under both normoxic (IC_{50} in the range 1.30 – 10.88 μM) and hypoxic (IC_{50} in the range 1.50 – 7.57 μM) conditions. In particular, compounds **2a** and **2h** were found to be the most potent of the series against HCT-116 cells under hypoxic conditions with IC_{50} values of 1.50±0.53 and 2.73±0.14 μM, respectively. In contrast, compounds **2a** and **2d** emerged as the most potent derivatives against A549 cells under both normoxic (IC_{50} = 3.53±0.16 and 4.77±0.22 μM, respectively) and hypoxic (IC_{50} = 2.68±0.31 and 5.74±0.28 μM, respectively) conditions. Compound **2d**, instead, showed the best growth inhibitory activity against PC-3 cells with IC_{50} values of 6.31±0.41 and 0.82±0.06 μM under normoxic and hypoxic conditions, respectively.

The SAR outcomes illustrate that the substituents on the **BTD** scaffold such as in **2d**, **2h** and **2i** increase the growth inhibition action against prostate PC-3 cells compared to the unsubstituted **2a**. On the other hand, *N*-4 methylation (**2o**), produced a worsening of effectiveness against the three tested cancer cell lines in comparison to *N*-4 unsubstituted analogue **2a**. Notably, such methylation decreased the CA IX and XII inhibitory activities as well.

Additionally, compounds **2a**, **2d**, **2h**, **2i** and **2o** were examined for their cytotoxic effect toward the non-tumorigenic lung fibroblast WI-38 cell line to investigate their safety profile (Table 3). The examined **BTDs** displayed significantly minor cytotoxic impact against the non-tumorigenic cell line when compared to HCT116 cells with IC_{50} in the range 23.5 ± 0.8 – 124.6±3.6 μM. Derivatives **2a** and **2h** stood out among the others for a good safety profile with *SI* of 30.7 and 32.3, respectively (Table 3).

Table 3. *In vitro* cytotoxic activity of **BTDs 2a**, **2d**, **2h**, **2i** and **2o** against non-tumorigenic WI-38 cells, and WI-38/HCT116 *SI*.

Compound	IC_{50} WI-38 (μM)[a]	*SI* WI-38/HCT116
2a	39.9 ± 1.4	30.7
2d	23.5 ± 0.8	6.1
2h	124.6 ± 3.6	32.3
2i	36.6 ± 1.8	7.0
2o	40.89 ± 3.2	3.8

a. IC_{50} values are the mean ± S.D. of three separate experiments.

2.3.1. Effects on the levels of apoptotic markers

The ability of **2a** and **2h** to provoke apoptosis in colon HCT-116 cells was assessed by measuring the expression levels of apoptosis hallmark parameters upon treatment with the compounds at their IC_{50} concentrations (1.30 and 3.86 μM, respectively) (Figure 6, Tables S3 and S4). The exposure of HCT-116 cells to **2a** and **2h** induced a significant down-regulation of the expression levels of the anti-apoptotic protein Bcl-2 by approximately 59% and 42%, respectively, with a concurrent 8.12- and 4.73-fold increase, respectively, in the expression of the

pro-apoptotic protein Bax, compared to the control. Accordingly, the Bax/Bcl-2 ratio was calculated to be boosted by 21.4- and 8.6-fold, respectively, in comparison to the control (Figure 6 and Table S4, Supporting Information).

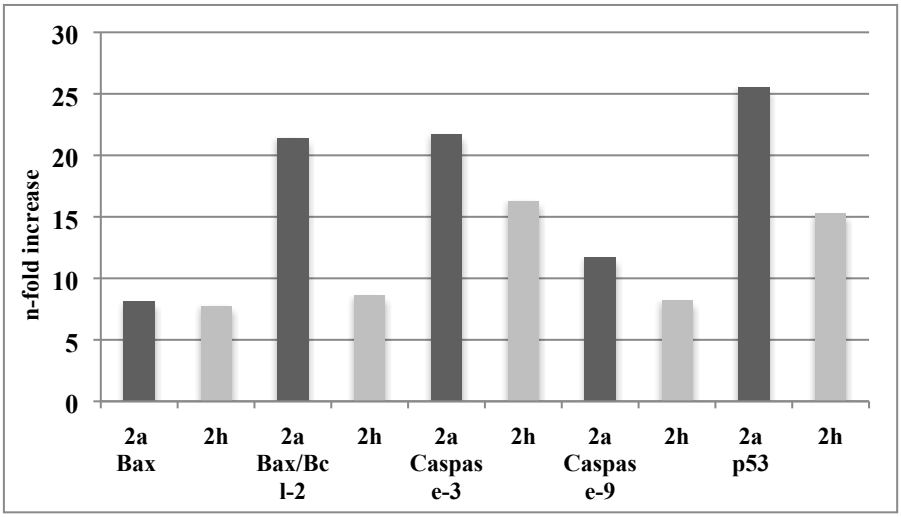

Figure 6. Increase in Bax/Bcl-2 ratio and expression levels of Bax, caspase-3, caspase-9, and p53 in HCT116 cancer cells upon treatment with **2a** and **2h** in comparison to the control.

Thereafter, the expression levels of active caspase-3, caspase-9 and p53 tumor suppressor protein were evaluated. Treatment of HCT-116 cells with **2a** and **2h** led to a significant increase in the expression levels of the pro-apoptotic caspase-3 (by 21.7- and 16.3-fold, respectively), caspase-9 (by 11.7- and 8.2-fold, respectively), and p53 (by 25.5- and 15.3-fold, respectively), compared to control (Figure 6 and Table S5, Supporting Information).

3. Conclusions

After their kinetical and structural characterization as selective inhibitors of the tumor-associated CAs IX and XII, the sweeteners **SAC** and **ACE** have entered the topic of anticancer CAIs. Here, a drug design strategy over the structures of **SAC** and **ACE** was reported, which produced a new series of 2H-benzo[e][1,2,4]thiadiazin-3(4H)-one 1,1-dioxides (**BTD**). Many such derivatives showed enhanced potency (CA IX K_Is in the range 19.1-408.5 nM; CA XII K_Is in the range 15.5-764.0 nM) and in some cases selectivity (II/IX selectivity index between 2 and 76; II/XII selectivity index between 2 and 440) when compared to the leads against the target CA IX and XII

over off-target isoforms. A thorough X-ray crystallographic study conducted on 5 derivatives with both CA II and IX-mimic enabled the speculation that the larger hydrophobic pocket in CA IX compared to CA II, along which substrate and many inhibitors travel, facilitates the binding of bulkier, aromatic compounds such as these ureidosulfonamides. A subset of compounds selected for the *in vitro* evaluation of their anticancer properties (**2a**, **2d**, **2h**, **2i** and **2o**) exhibited a greater efficacy against colon HCT-116 than A549 and PC-3 cells, except **2d** and **2i** which displayed an enhanced growth inhibition against PC-3 cells under the hypoxic conditions. In particular, **BTDs 2a** and **2h** (IC_{50} against HCT-116 cells of 1.30±0.06 and 3.86±0.19 μM in normoxia, and 1.50±0.53 and 2.73±0.14 μM in hypoxia, respectively) were selected to further assess their effect on apoptosis markers in HCT-116 cells. Treatment with **2a** and **2h** led to a significant increase in the expression levels of the pro-apoptotic proteins Bax, caspase-3, caspase-9, and p53 and a down-regulation of the anti-apoptotic protein Bcl-2. These outcomes indicate that **SAC** and **ACE**, widely used as sweeteners might be used for designing promising leads for the development of new anticancer drugs.

4. Experimental Section

4.1 Chemistry

Anhydrous solvents and all reagents were purchased from Sigma-Aldrich (Milan, Italy), Alfa Aesar (Milan, Italy) and TCI (Milan, Italy). All reactions involving air- or moisture-sensitive compounds were performed under a nitrogen atmosphere using dried glassware and syringes techniques to transfer solutions. Nuclear magnetic resonance spectra (^{1}H-NMR: 400 MHz; ^{13}C-NMR: 100 MHz; ^{19}F-NMR: 376 MHz) were recorded in DMSO-d_6 using an Avance III 400 MHz spectrometer (Bruker, Milan, Italy). Chemical shifts are reported in parts per million (ppm) and the coupling constants (*J*) are expressed in Hertz (Hz). Splitting patterns are designated as follows: s, singlet; d, doublet; t, triplet; q, quadruplet; m, multiplet; brs, broad singlet; dd, double of doublets. The

assignment of exchangeable protons (OH and NH) was confirmed by the addition of D_2O. Analytical thin-layer chromatography (TLC) was carried out on silica gel F-254 plates (Merck, Milan, Italy). Flash chromatography purifications were performed on Merck Silica gel 60 (230-400 mesh ASTM) as the stationary phase and ethyl acetate/n-hexane were used as eluents. Melting points (m.p.) were carried out in open capillary tubes and are uncorrected.

The HPLC analysis was performed by using an Agilent 1200 Series equipped by autosampler, binary pump system and diode array detector (DAD). The column used was a Luna PFP 30 mm length, 2 mm internal diameter and 3 μm particle size (Phenomenex, Bologna, Italy) at constant flow of 0.25 mL min^{-1}, employing a binary mobile phase elution gradient. The eluents used were 10 mM formic acid and 5 mM ammonium formate in mQ water solution (solvent A) and 10 mM formic acid and 5 mM ammonium formate in methanol (solvent B) according to the elution gradient as follows: initial at 90% solvent A, which was then decreased to 10% in 8 min, kept for 3 min, returned to initial conditions in 0.1 min and maintained for 3 min for reconditioning, to a total run time of 14 min. The stock solution of each analyte was prepared in methanol at 1.0 mg mL^{-1} and stored at 4 °C. The sample solution of the analyte was freshly prepared by diluting its stock solution up to a concentration of 10 μg mL^{-1} in mixture of mQ water:methanol 50:50 (v/v) and 5 μL were injected in the HPLC system. All compounds reported were >95% HPLC pure. The solvents used in HPLC measures were methanol (Chromasolv grade), purchased from Sigma-Aldrich (Milan - Italy), and mQ water 18 MΩ cm, obtained from Millipore's Simplicity system (Milan-Italy).

High resolution mass spectrometry (HR-MS) analysis was performed with a Thermo Finnigan LTQ Orbitrap mass spectrometer equipped with an electrospray ionization source (ESI). Analysis were carried out in negative ion mode monitoring the $[M-H]^-$ species, and a proper dwell time acquisition was used to achieve 60,000 units of resolution at Full Width at Half Maximum (FWHM). Elemental composition of compounds were calculated on the basis of their measured accurate masses, accepting only results with an attribution error less than 5 ppm and a not integer RDB (double

bond/ring equivalents) value, in order to consider only the deprotonated species.[32] None of the screened derivatives reported PAINS alerts determined by SwissADME server (www.swissadme.ch).

General procedure for the synthesis of compounds 2a-q.

A solution of chlorosulfonyl isocyanate (0.48 mL, 1.1 eq.) in the proper solvent (nitromethane or nitroethane) was treated with a solution of the appropriate aromatic amine (1.0 eq.) in the same solvent (5 mL) at –40 °C. The reaction mixture was stirred for 15 min before $AlCl_3$ (1.0 eq.) was added and then it was warmed at 110 °C and stirred for 45 min. The resulting mixture was cooled and poured onto ice. The formed precipitate was collected by filtration and dried to obtain a powder that was purified by silica gel column chromatography eluting with appropriate mixture of solvents or alternatively by dissolution in a saturated solution of $NaHCO_3$ in 1:1 H_2O/MeOH, treatment with charcoal, filtration over Celite and re-acidification to pH 1. The precipitate was filtered *in vacuo* to afford the titled compounds **2a-q**.

2H-Benzo[e][1,2,4]thiadiazin-3(4H)-one 1,1-dioxide (2a)

Compound **2a** was obtained according to the general procedure earlier reported adding dropwise a solution of aniline (0.46 mL, 1.0 eq.) in nitromethane (6.0 mL) to a solution of chlorosulfonyl isocyanate (0.48 mL, 1.12 eq.) in nitromethane (6.0 mL). The crude compound was purified by dissolution in a saturated solution of $NaHCO_3$ in 1:1 H_2O/MeOH, treatment with charcoal, filtration over Celite and re-acidification to pH 1. The precipitate was filtered *in vacuo* to afford the title compound **2a**. 31% yield; m.p. >300°C; TLC: R_f = 0.30 (methanol/dichloromethane 20% *v/v*); ^{1}H-NMR (DMSO-d_6, 400 MHz): δ 7.27 (2H, m, Ar-*H*), 7.64 (1H, t, J = 8.0, Ar-*H*), 7.78 (1H, d, J = 7.6, Ar-*H*), 11.09 (1H, s, exchange with D_2O, CON*H*); ^{13}C-NMR (DMSO-d_6, 100 MHz): δ 117.7,

122.9, 123.5, 124.1, 134.6, 136.2, 151.9; ESI-HRMS (m/z) $[M-H]^-$: calculated for C7H5N2O3S 197.0021; found 197.0028.

5-Methyl-2H-benzo[e][1,2,4]thiadiazin-3(4H)-one 1,1-dioxide (2b)

Compound **2b** was obtained according to the general procedure earlier reported adding dropwise a solution of *o*-toluidine (1.0 g., 1.0 eq.) in nitroethane (8.0 mL) to a solution of chlorosulfonyl isocyanate (0.89 mL, 1.1 eq.) in nitroethane (7.0 mL). The crude compound was purified by dissolution in a saturated solution of $NaHCO_3$ in 1:1 H_2O/MeOH, treatment with charcoal, filtration over Celite and re-acidification to pH 1. The precipitate was filtered *in vacuo* to afford **2b**. 26% yield; m.p. 292-293°C; TLC: R_f = 0.13 (methanol/dichloromethane 15% *v/v*); ^{1}H-NMR (DMSO-d_6, 400 MHz): δ 2.40 (3H, s, CH_3), 7.25 (1H, t, J = 7.6, Ar-*H*), 7.55 (1H, d, J = 7.6, Ar-*H*), 7.66 (1H, d, J = 7.6, Ar-*H*), 10.42 (1H, s, exchange with D_2O, CON*H*); ^{13}C-NMR (DMSO-d_6, 100 MHz): δ 18.4, 120.4, 124.1, 124.4, 127.3, 134.1, 136.1, 151.6; ESI-HRMS (m/z) $[M-H]^-$: calculated for C8H7N2O3S 211.0177; found 211.0181.

7-Methyl-2H-benzo[e][1,2,4]thiadiazin-3(4H)-one 1,1-dioxide (2c)

Compound **2c** was obtained according to the general procedure earlier reported adding dropwise a solution of p-toluidine (1.0 g., 1.0 eq.) in nitromethane (9.7 mL) to a solution of chlorosulfonyl isocyanate (0.60 mL, 1.2 eq.) in nitromethane (6.4 mL). The crude compound was purified by dissolution in a saturated solution of $NaHCO_3$ in 1:1 H_2O/MeOH, treatment with charcoal, filtration over Celite and re-acidification to pH 1. The precipitate was filtered *in vacuo* to afford **2c** as a white solid. 40% yield; m.p. 287-288°C; TLC: R_f = 0.30 (methanol/dichloromethane 30% *v/v*); ^{1}H-NMR (DMSO-d_6, 400 MHz): δ 2.38 (3H, s, CH_3), 7.17 (1H, d, J = 8.4, Ar-*H*), 7.49 (1H, dd, J = 8.0, 1.2, Ar-*H*), 7.63 (1H, s, Ar-*H*), 11.18 (1H, s, exchange with D_2O, CON*H*); ^{13}C-NMR (DMSO-d_6, 100

MHz): δ 21.0, 117.8, 122.4, 123.3, 133.6, 134.0, 135.6, 151.5; ESI-HRMS (m/z) $[M-H]^-$: calculated for C8H7N2O3S 211.0177; found 211.0169.

5,7-Dimethyl-2H-benzo[e][1,2,4]thiadiazin-3(4H)-one 1,1-dioxide (2d)

Compound **2d** was obtained according to the general procedure earlier reported adding dropwise a solution of 2,4-dimenthylaniline (1.02 mL, 1.0 eq.) in nitromethane (5.0 mL) to a solution of chlorosulfonyl isocyanate (0.93 mL, 1.3 eq.) in nitromethane (5.0 mL). The crude compound was purified by dissolution in a saturated solution of $NaHCO_3$ in 1:1 H_2O/MeOH, treatment with charcoal, filtration over Celite and re-acidification to pH 1. The precipitate was filtered *in vacuo* to afford **2d** as a white solid. 60% yield; m.p. 290-291°C; TLC: R_f = 0.23 (methanol/dichloromethane 20% *v/v*); ^{1}H-NMR (DMSO-d_6, 400 MHz): δ 2.35 (6H, d, J = 5.6, 2 x CH_3), 7.37 (1H, s, Ar-*H*), 7.48 (1H, s, Ar-*H*), 10.35 (1H, s, exchange with D_2O, CON*H*); ^{13}C-NMR (DMSO-d_6, 100 MHz): δ 18.3, 20.7, 119.9, 124.3, 127.1, 131.7, 133.7, 136.9, 151.5; ESI-HRMS (m/z) $[M-H]^-$: calculated for C9H9N2O3S 225.0334; found 225.0329.

5,8-Dimethyl-2H-benzo[e][1,2,4]thiadiazin-3(4H)-one 1,1-dioxide (2e)

Compound **2e** was obtained according to the general procedure earlier reported adding dropwise a solution of 2,5-dimenthylaniline (1.03 mL, 1.0 eq.) in nitromethane (8.0 mL) to a solution of chlorosulfonyl isocyanate (0.93 mL, 1.3 eq.) in nitromethane (7.0 mL). The crude compound was purified by dissolution in a saturated solution of $NaHCO_3$ in 1:1 H_2O/MeOH, treatment with charcoal, filtration over Celite and re-acidification to pH 1. The precipitate was filtered *in vacuo* to afford **2e** as a white solid. 66% yield; m.p. 297-298°C; TLC: R_f = 0.16 (methanol/dichloromethane 20% *v/v*); ^{1}H-NMR (DMSO-d_6, 400 MHz): δ 2.35 (3H, s, 5-CH_3), 2.57 (3H, s, 8-CH_3), 7.04 (1H, d, J = 7.6, Ar-*H*), 7.38 (1H, d, J = 8.0, Ar-*H*), 10.17 (1H, s, exchange with D_2O, CON*H*); ^{13}C-NMR

(DMSO-d_6, 100 MHz): δ 18.4, 20.0, 123.2, 124.6, 126.7, 132.9, 134.4, 135.1, 151.2; ESI-HRMS (m/z) $[M-H]^-$: calculated for C9H9N2O3S 225.0334; found 225.0338.

6,8-Dimethyl-2H-benzo[e][1,2,4]thiadiazin-3(4H)-one 1,1-dioxide (2f)

Compound **2f** was obtained according to the general procedure earlier reported adding dropwise a solution of 3,5-dimethylaniline (1.03 mL, 1.0 eq.) in nitromethane (5.0 mL) to a solution of chlorosulfonyl isocyanate (0.93 mL, 1.3 eq.) in nitromethane (5.0 mL). The crude compound was purified by dissolution in a saturated solution of $NaHCO_3$ in 1:1 H_2O/MeOH, treatment with charcoal, filtration over Celite and re-acidification to pH 1. The precipitate was filtered *in vacuo* to afford **2f** as a solid. 32% yield; m.p. 282-283°C; TLC: R_f = 0.11 (methanol/dichloromethane 20% *v/v*); ^{1}H-NMR (DMSO-d_6, 400 MHz): δ 2.32 (3H, s, 6-CH_3), 2.54 (3H, s, overlap with DMSO peak, 8-CH_3), 6.89 (1H, s, Ar-*H*), 6.95 (1H, s, Ar-*H*), 11.17 (1H, s, exchange with D2O, CON*H*); ^{13}C-NMR (DMSO-d_6, 100 MHz): δ 20.0, 21.9, 115.6, 119.7, 127.9, 135.5, 136.4, 144.2, 151.1; ESI-HRMS (m/z) $[M-H]^-$: calculated for C9H9N2O3S 225.0334; found 225.0341.

5-Fluoro-2H-benzo[e][1,2,4]thiadiazin-3(4H)-one 1,1-dioxide (2g)

Compound **2g** was obtained according to the general procedure earlier reported adding dropwise a solution of 2-fluoroaniline (0.87 mL, 1.0 eq.) in nitroethane (5.0 mL) to a solution of chlorosulfonyl isocyanate (0.94 mL, 1.2 eq.) in nitroethane (5.0 mL). The crude compound was purified by dissolution in a saturated solution of $NaHCO_3$ in 1:1 H_2O/MeOH, treatment with charcoal, filtration over Celite and re-acidification to pH 1. The precipitate was filtered *in vacuo* to afford **2g**. 10% yield; m.p. 277-278°C; TLC: R_f = 0.48 (ethyl acetate/*n*-hexane 70% *v/v*); ^{1}H-NMR (DMSO-d_6, 400 MHz): δ 7.34 (1H, m, Ar-*H*), 7.64 (2H, m, Ar-*H*), 11.31 (1H, s, exchange with D_2O, CON*H*); ^{13}C-NMR (DMSO-d_6, 100 MHz): δ 118.7 (J^3_{C-F} = 4 Hz), 120.5 (J^2_{C-F} = 18), 124.9 (J^3_{C-F} = 6), 125.2

($J^2_{C\text{-}F}$ = 15), 125.8, 150.2 ($J^1_{C\text{-}F}$ = 249), 151.5; ^{19}F-NMR (DMSO-d_6, 376 MHz) −125.93 (1F, s); ESI-HRMS (m/z) $[M\text{-}H]^-$: calculated for C7H4FN2O3S 214.9927; found 214.9935.

7-Fluoro-2H-benzo[e][1,2,4]thiadiazin-3(4H)-one 1,1-dioxide (2h)

Compound **2h** was obtained according to the general procedure earlier reported adding dropwise a solution of 4-fluoroaniline (1.0 g., 1.0 eq.) in nitromethane (5.0 mL) to a solution of chlorosulfonyl isocyanate (1.02 mL, 1.3 eq.) in nitromethane (5.0 mL). The crude compound was purified by dissolution in a saturated solution of $NaHCO_3$ in 1:1 H_2O/MeOH, treatment with charcoal, filtration over Celite and re-acidification to pH 1. The precipitate was filtered *in vacuo* to afford **2h** as a solid. 38% yield; m.p. 288-289°C; TLC: R_f = 0.28 (methanol/dichloromethane 30% *v/v*); ^{1}H-NMR (DMSO-d_6, 400 MHz): δ 7.32 (1H, m, Ar-*H*), 7.59 (1H, m, Ar-*H*), 7.72 (1H, m, Ar-*H*), 11.41 (1H, s, exchange with D_2O, CON*H*); ^{13}C-NMR (DMSO-d_6, 100 MHz): δ 109.6 ($J^2_{C\text{-}F}$ = 26), 120.3 ($J^2_{C\text{-}F}$ = 8), 122.5 ($J^3_{C\text{-}F}$ = 23), 124.1 ($J^2_{C\text{-}F}$ = 7), 132.7 ($J^4_{C\text{-}F}$ = 2), 152.1, 158.3 ($J^1_{C\text{-}F}$ = 242); ^{19}F-NMR (DMSO-d_6, 376 MHz) −117.29 (1F, s); ESI-HRMS (m/z) $[M\text{-}H]^-$: calculated for C7H4FN2O3S 214.9927; found 214.9921.

5-Chloro-2H-benzo[e][1,2,4]thiadiazin-3(4H)-one 1,1-dioxide (2i)

Compound **2i** was obtained according to the general procedure earlier reported adding dropwise a solution of 2-chloraniline (0.82 mL, 1.0 eq.) in nitroethane (6.0 mL) to a solution of chlorosulfonyl isocyanate (0.89 mL, 1.3 eq.) in nitroethane (6.0 mL). The crude compound was purified by dissolution in a saturated solution of $NaHCO_3$ in 1:1 H_2O/MeOH, treatment with charcoal, filtration over Celite and re-acidification to pH 1. The precipitate was filtered *in vacuo* to afford **2i** as a white solid. 34% yield; m.p. 246-247°C; TLC: R_f = 0.08 (methanol/dichloromethane 10% *v/v*); ^{1}H-NMR (DMSO-d_6, 400 MHz): δ 7.36 (1H, t, J = 8.0, Ar-*H*), 7.85 (2H, m, Ar-*H*), 10.71 (1H, s, exchange

with D_2O, CON*H*); ^{13}C-NMR (DMSO-d_6, 100 MHz): δ 121.5, 122.0, 125.4, 126.1, 133.1, 135.1, 151.4; ESI-HRMS (m/z) $[M-H]^-$: calculated for C7H4ClN2O3S 230.9631; found 230.9626.

7-Chloro-2H-benzo[e][1,2,4]thiadiazin-3(4H)-one 1,1-dioxide (2j)

Compound **2j** was obtained according to the general procedure earlier reported adding dropwise a solution of 4-chloroaniline (1.0 g, 1.0 eq.) in nitroethane (6.0 mL) to a solution of chlorosulfonyl isocyanate (0.82 mL, 1.2 eq.) in nitroethane (6.0 mL). The crude compound was purified by dissolution in a saturated solution of $NaHCO_3$ in 1:1 H_2O/MeOH, treatment with charcoal, filtration over Celite and re-acidification to pH 1. The precipitate was filtered *in vacuo* to afford **2j** as a solid. 48% yield; m.p. 285-286°C; TLC: R_f = 0.11 (methanol/dichloromethane 15% *v/v*); ^{1}H-NMR (DMSO-d_6, 400 MHz): δ 7.30 (1H, d, J = 8.8, Ar-*H*), 7.74 (1H, t, J = 8.0, 2.4, Ar-*H*), 7.86 (1H, d, J = 2.0, Ar-*H*), 11.47 (1H, s, exchange with D_2O, CON*H*); ^{13}C-NMR (DMSO-d_6, 100 MHz): δ 120.1, 122.6, 124.5, 128.1, 134.7, 135.0, 152.0; ESI-HRMS (m/z) $[M-H]^-$: calculated for C7H4ClN2O3S 230.9631; found 230.9636.

5-Bromo-2H-benzo[e][1,2,4]thiadiazin-3(4H)-one 1,1-dioxide (2k)

Compound **2k** was obtained according to the general procedure earlier reported adding dropwise a solution of 2-bromoaniline (1.0 g, 1.0 eq.) in nitroethane (5.0 mL) to a solution of chlorosulfonyl isocyanate (0.61 mL, 1.2 eq.) in nitroethane (5.0 mL). The crude compound was purified by dissolution in a saturated solution of $NaHCO_3$ in 1:1 H_2O/MeOH, treatment with charcoal, filtration over Celite and re-acidification to pH 1. The precipitate was filtered *in vacuo* to afford **2k** as a solid. 25% yield; m.p. 250-251°C; TLC: R_f = 0.19 (methanol/dichloromethane 15% *v/v*); ^{1}H-NMR (DMSO-d_6, 400 MHz): δ 7.29 (1H, t, J = 8.0, Ar-*H*), 7.86 (1H, d, J = 7.2 Ar-*H*), 8.00 (1H, dd, J = 8.4, 1.2, Ar-*H*), 10.28 (1H, s, exchange with D_2O, CON*H*); ^{13}C-NMR (DMSO-d_6, 100 MHz): δ

111.1, 122.6, 125.8, 126.2, 134.2, 138.4, 151.4; ESI-HRMS (m/z) $[M-H]^-$: calculated for C7H4BrN2O3S 274.9126; found 274.9120.

7-Bromo-2H-benzo[e][1,2,4]thiadiazin-3(4H)-one 1,1-dioxide (2l)

Compound **2l** was obtained according to the general procedure earlier reported adding dropwise a solution of 4-bromoaniline (1.0 g., 1.0 eq.) in nitromethane (5.0 mL) to a solution of chlorosulfonyl isocyanate (0.60 mL, 1.2 eq.) in nitromethane (5.0 mL). The crude compound was purified by dissolution in a saturated solution of $NaHCO_3$ in 1:1 H_2O/MeOH, treatment with charcoal, filtration over Celite, re-acidification to pH 1. The precipitate was filtered *in vacuo* to afford **2l** as a white solid. 30% yield; m.p. >300°C; TLC: R_f = 0.11 (methanol/dichloromethane 20% *v/v*); ^{1}H-NMR (DMSO-d_6, 400 MHz): δ 7.24 (1H, d, *J* = 8.8, Ar-*H*), 7.85 (1H, dd, *J* =8.8, 2.2, Ar-*H*), 7.95 (1H, d, *J* = 2.0, Ar-*H*), 11.46 (1H, s, exchange with D_2O, CON*H*); ^{13}C-NMR (DMSO-d_6, 100 MHz): 115.5, 120.3, 124.9, 125.2, 135.4, 137.4, 152.0; ESI-HRMS (m/z) $[M-H]^-$: calculated for C7H4BrN2O3S 274.9126; found 274.9130.

7-Methoxy-2H-benzo[e][1,2,4]thiadiazin-3(4H)-one 1,1-dioxide (2m)

Compound **2m** was obtained according to the general procedure earlier reported adding dropwise a solution of p-anisidine (1.0 g, 1.0 eq.) in nitromethane (4.0 mL) to a solution of chlorosulfonyl isocyanate (0.78 mL, 1.1 eq.) in nitromethane (5.7 mL). The crude compound was purified by silica gel column chromatography eluting with from 1 to 15% *v/v* MeOH/DCM to give a residue which was further purified by dissolution in a saturated solution of $NaHCO_3$ in 1:1 H_2O/MeOH, treatment with charcoal, filtration over Celite, re-acidification to pH 1. The precipitate was filtered *in vacuo* to afford **2m** as a solid. 17% yield; m.p. 284-285°C; TLC: R_f = 0.15 (methanol/dichloromethane 5% *v/v*); ^{1}H-NMR (DMSO-d_6, 400 MHz): δ 3.85 (3H, s, CH_3), 7.26 (3H, m, Ar-*H*), 11.15 (1H, s, exchange with D_2O, CON*H*); ^{13}C-NMR (DMSO-d_6, 100 MHz): δ 56.9, 105.5, 119.7, 122.7, 123.9,

129.5, 151.8, 156.1; ESI-HRMS (m/z) $[M-H]^-$: calculated for C8H7N2O4S 227.0127; found 227.0122.

1H-Naphtho[1,2-e][1,2,4]thiadiazin-2(3H)-one 4,4-dioxide (2n)

Compound **2n** was obtained according to the general procedure earlier reported adding dropwise a solution of 1-naphthylamine (1.0 g, 1.0 eq.) in nitroethane (5.0 mL) to a solution of chlorosulfonyl isocyanate (0.67 mL, 1.1 eq.) in nitroethane (5.0 mL). The crude compound was purified by dissolution in a saturated solution of $NaHCO_3$ in 1:1 H_2O/MeOH, treatment with charcoal, filtration over Celite and re-acidification to pH 1. The precipitate was filtered *in vacuo* to afford a green semisolid, that was purified by silica gel column chromatography eluting with 60 to 100% EtOAc/n-hexane to give **2n**. 3% yield; m.p. 293-294°C; TLC: R_f = 0.15 (methanol/dichloromethane 15% *v/v*); ^{1}H-NMR (DMSO-d_6, 400 MHz): δ 7.76 (3H, m, Ar-*H*), 7.86 (1H, d, J = 8.8, Ar-*H*), 8.08 (1H, d, J = 7.6, Ar-*H*), 8.72 (1H, d, J = 8.0, Ar-*H*), 11.34 (1H, s, exchange with D_2O, CON*H*); ^{13}C-NMR (DMSO-d_6, 100 MHz): δ 118.4, 118.8, 122.6, 123.7, 124.7, 128.5, 129.7, 129.9, 133.1, 135.9, 152.2; ESI-HRMS (m/z) $[M-H]^-$: calculated for C11H7N2O3S 247.0177; found 247.0183.

4-Methyl-2H-benzo[e][1,2,4]thiadiazin-3(4H)-one 1,1-dioxide (2o)

Compound **2o** was obtained according to the general procedure earlier reported adding dropwise a solution of *N*-methylaniline (1.01 mL, 1.0 eq.) in nitroethane (5.0 mL) to a solution of chlorosulfonyl isocyanate (0.90 mL, 1.1 eq.) in nitroethane (5.0 mL). The crude compound was purified by dissolution in a saturated solution of $NaHCO_3$ in 1:1 H_2O/MeOH, treatment with charcoal, filtration over Celite and re-acidification to pH 1. The precipitate was filtered *in vacuo* to afford **2o** as a solid. 27% yield; m.p. 257-258°C; TLC: R_f = 0.20 (methanol/dichloromethane 15% *v/v*); ^{1}H-NMR (DMSO-d_6, 400 MHz): δ 3.47 (3H, s, CH_3), 7.42 (1H, t, J = 7.4, Ar-*H*), 7.56 (1H, d, J = 8.4, Ar-*H*), 7.81 (1H, m, Ar-*H*), 7.89 (1H, dd, J = 8.0, 1.2, Ar-*H*); ^{13}C-NMR (DMSO-d_6, 100

MHz): δ 32.5, 117.9, 122.7, 124.4, 126.1, 135.2, 137.9, 151.2; ESI-HRMS (m/z) $[M-H]^-$: calculated for C8H7N2O3S 211.0177; found 211.0182.

7-Chloro-4-methyl-2H-benzo[e][1,2,4]thiadiazin-3(4H)-one 1,1-dioxide (2p)

Compound **2p** was obtained according to the general procedure earlier reported adding dropwise a solution of 4-chloro-*N*-methylaniline (0.86 mL, 1.0 eq.) in nitroethane (6.0 mL) to a solution of chlorosulfonyl isocyanate (0.74 mL, 1.2 eq.) in nitroethane (6.0 mL). The crude compound was purified by dissolution in a saturated solution of $NaHCO_3$ in 1:1 H_2O/MeOH, treatment with charcoal, filtration over Celite and re-acidification to pH 1. The precipitate was filtered *in vacuo* to afford **2p** as a white solid. 29% yield; m.p. 254-255°C; TLC: R_f = 0.20 (methanol/dichloromethane 15% *v/v*); ^{1}H-NMR (DMSO-d_6, 400 MHz): δ 3.33 (3H, m, overlap with water peak, CH_3), 7.57 (1H, d, J = 9.2, Ar-*H*), 7.85 (1H, dd, J = 6.4, 2.4, Ar-*H*), 7.94 (1H, d, J = 2.4); ^{13}C-NMR (DMSO-d_6, 100 MHz): δ 32.8, 120.1, 122.2, 127.4, 128.4, 134.8, 137.1, 151.2; ESI-HRMS (m/z) $[M-H]^-$: calculated for C8H6ClN2O3S 244.9788; found 244.9782.

5,6-Dihydro-[1,2,4]thiadiazino[6,5,4-hi]indol-3(2H)-one 1,1-dioxide (2q)

Compound **2q** was obtained according to the general procedure earlier reported adding dropwise a solution of indoline (0.94 mL, 1.0 eq.) in nitroethane (6.0 mL) to a solution of chlorosulfonyl isocyanate (0.95 mL, 1.3 eq.) in nitroethane (6.0 mL). The crude compound was purified by dissolution in a saturated solution of $NaHCO_3$ in 1:1 H_2O/MeOH, treatment with charcoal, filtration over Celite and re-acidification to pH 1. The precipitate was filtered *in vacuo* to afford **2q** as a solid. 68% yield; m.p. 252-253°C; TLC: R_f = 0.15 (methanol/dichloromethane 15% *v/v*); ^{1}H-NMR (DMSO-d_6, 400 MHz): δ 3.34 (2H, t, J = 8.6, CH_2), 4.17 (2H, t, J = 8.4, CH_2), 7.26 (1H, t, J = 7.6, Ar-*H*), 7.62 (2H, t, J = 8.6, Ar-*H*); ^{13}C-NMR (DMSO-d_6, 100 MHz): δ 28.0, 47.8, 119.6, 120.9,

124.9, 130.7, 133.4, 139.4, 149.2; ESI-HRMS (m/z) $[M-H]^-$: calculated for C9H7N2O3S 223.0177; found 223.0173.

3-Oxo-3,4-dihydro-2H-benzo[e][1,2,4]thiadiazine-5-carboxylic acid 1,1-dioxide (2r)

Compound **2b** (0.5 g, 1.0 eq.) was first suspended in H_2O (30 mL) and then dissolved during the addition of saturated aqueous NaOH (0.56 g). $KMnO_4$ (1.42 g, 3.8 eq.) was added portionwise at 0°C, and the reaction mixture was stirred at 80°C for 12 h. The insoluble material was removed by filtration, and the filtrate was acidified to pH 1 with concentrated HCl. The precipitate was collected by filtration, washed with Et_2O, and dried to yield the product **2r** as a white solid. 33% yield; m.p. 285-286°C; TLC: R_f = 0.14 (methanol/dichloromethane 20% *v/v*); ^{1}H-NMR (DMSO-d_6, 400 MHz): δ 7.26 (1H, t, J = 7.8, Ar-*H*), 7.97 (1H, d, J = 7.6, Ar-*H*), 8.18 (1H, dd, J = 8.0, 0.8, Ar-*H*), 10.58 (1H, s, exchange with D_2O, CON*H*), 14.01 (1H, s, exchange with D_2O, COO*H*); ^{13}C-NMR (DMSO-d_6, 100 MHz): δ 114.7, 122.1, 125.1, 128.8, 135.5, 139.0, 152.5, 169.3; ESI-HRMS (m/z) $[M-H]^-$: calculated for C8H5N2O5S 240.9919; found 240.9911.

3-Oxo-3,4-dihydro-2H-benzo[e][1,2,4]thiadiazine-7-carboxylic acid 1,1-dioxide (2s)

Compound **2c** (0.2 g, 1.0 eq.) was first suspended in H_2O (12 mL) and then dissolved during the addition of saturated aqueous NaOH (0.23 g). $KMnO_4$ (0.49 g, 3.3 eq.) was added portionwise at 0°C, and the reaction mixture was stirred at 80°C for 7 h. The insoluble material was removed by filtration, and the filtrate was acidified to pH 1 with concentrated HCl. The precipitate was collected by filtration, washed with acid water and Et_2O, and dried to yield the product **2s** as a white solid. 21% yield; m.p. >300°C; TLC: R_f = 0.17 (methanol/dichloromethane 20% *v/v*); ^{1}H-NMR (DMSO-d_6, 400 MHz): δ 7.37 (1H, d, J = 8.4, Ar-*H*), 8.19 (1H, m, Ar-*H*), 8.23 (1H, s, Ar-*H*), 11.64 (1H, s, exchange with D_2O, CON*H*), 13.38 (1H, s, exchange with D_2O, O*H*); ^{13}C-NMR (DMSO-d_6, 100

MHz): δ 118.3, 123.2, 124.4, 126.6, 135.4, 139.5, 151.8, 166.4; ESI-HRMS (m/z) $[M-H]^-$: calculated for C8H5N2O5S 240.9919; found 240.9923.

7-Hydroxy-2H-benzo[e][1,2,4]thiadiazin-3(4H)-one 1,1-dioxide (2t)

A solution of **2m** (0.2 g, 1.0 eq.) in dichloromethane (15 mL) was treated with BBr_3 (1.84 mL, 3.0 eq.) at –10 °C. The reaction mixture was stirred for 12 h at r.t. After completion of the reaction, the mixture was quenched with ice and the dichloromethane was evaporated under *vacuum*. The suspended solid was filtered *in vacuo* to afford **2t** as a solid. 42% yield; m.p. 284-285°C; TLC: R_f= 0.56 (methanol/dichloromethane 30% *v/v*); ^{1}H-NMR (DMSO-d_6, 400 MHz): δ 7.12 (3H, m, Ar-*H*), 10.03 (1H, s, exchange with D_2O, O*H*), 11.04 (1H, s, exchange with D_2O, CON*H*), 12.67 (1H, s, exchange with D_2O, SO_2N*H*); ^{13}C-NMR (DMSO-d_6, 100 MHz): 107.3, 119.6, 122.8, 124.0, 127.9, 151.7, 154.2; ESI-HRMS (m/z) $[M-H]^-$: calculated for C7H5N2O4S 212.9970; found 212.9974.

4.2. Carbonic anhydrases inhibition

An Applied Photophysics stopped-flow instrument has been used for assaying the CA catalysed CO_2 hydration activity.[23] Phenol red (at a concentration of 0.2 mM) has been used as indicator, working at the absorbance maximum of 557 nm, with 20 mM Hepes (pH 7.5) as buffer, and 20 mM Na_2SO_4 (for maintaining constant the ionic strength), following the initial rates of the CA-catalysed CO_2 hydration reaction for a period of 10–100 s. The CO_2 concentrations ranged from 1.7 to 17 mM for the determination of the kinetic parameters and inhibition constants. For each inhibitor at least six traces of the initial 5–10% of the reaction have been used for determining the initial velocity. The uncatalyzed rates were determined in the same manner and subtracted from the total observed rates. Stock solutions of inhibitor (0.1 mM) were prepared in distilled-deionized water and dilutions up to 0.01 nM were done thereafter with the assay buffer. Inhibitor and enzyme solutions were preincubated together for 1 h at room temperature prior to assay, in order to allow for the formation

of the E-I complex. The inhibition constants were obtained by non-linear least-squares methods using PRISM 3 and the Cheng-Prusoff equation, as reported earlier,[33,34] and represent the mean from at least three different determinations. All CA isoforms were recombinant ones obtained in-house as reported earlier.[35]

4.3. X-ray crystallography

CA II and CA IX-mimic were expressed and purified as previously described.[36] The CA IX-mimic was produced by mutating 7 residues in the active site of CA II in order to mimic the active site of CA IX, resulting in a construct that is more easily expressed, purified, and crystallized than wild type hCA IX.[36] CA II and CA IX were expressed in BL21(DE3) *E. coli* cells induced by IPTG. The cells were then harvested and lysed for purification via affinity chromatography with p-(aminomethyl)benzenesulfonamide resin. Protein purity was confirmed vis SDS-PAGE and both CA II and CA IX were diluted to a final concentration of 10 mg/mL for crystallization. Crystals were subsequently grown using the hanging drop vaporization method with a precipitant solution of 1.6 M NaCitrate, 50 mM Tris, pH 7.8. Crystals were soaked in mM concentrations of the inhibitors before transferring to a cryoprotectant of 20% glycerol and freezing in liquid nitrogen.

Diffraction data was collected on the F1 beamline at Cornell High Energy Synchrotron Source (CHESS) using a Pilatus 6M detector. Data sets were collected with a crystal-to-detector distance of 250 mm, 1° oscillation angle, and exposure time of 2-3 sec for a total of 180 images. *XDS*[37] was used to index and integrate the data followed by *Aimless*[38] to scale the data to the $P2_1$ space group. The phases were then determined by molecular replacement with a search model of CA II (PDB: 3KS3[39]) and refinements performed in *Phenix*[40]. *Coot*[41] was used to analyze inhibitor interactions and *PyMol*[42] to generate figures.

4.4. Anticancer Activity

4.4.1. Antiproliferative activity

The three tested cancer cell lines (A549, PC-3 and HCT116), in addition to the non-tumorigenic lung fibroblast WI-38 cell line, were obtained from American Type Culture Collection (ATCC). The cells were propagated in DMEM supplemented with 10% heat-inactivated fetal bovine serum, 1% L-glutamine (2.5 mM), HEPES buffer (10 mM) and gentamycin (50 μg/mL). The hypoxia inducer $CoCl_2$ (100 μM) was added to achieve hypoxic conditions. All cells were maintained at 37 °C in a humidified atmosphere with CO_2 (5%). Cytotoxicity was then evaluated following the MTT assay[30], as described earlier.[43]

4.4.2. ELISA Immunoassay

The expression levels of the pro-apoptotic markers (Bax, caspase-3, caspase-9 and p53), in addition to the anti-apoptotic marker (Bcl-2) were evaluated using ELISA colorimetric kits per the manufacturer's instructions, as reported previously.[43,44]

Acknowledgements

MIUR is gratefully acknowledged for a grant to A.N (PRIN: rot. 2017XYBP2R). This work was in part funded by the Researchers Supporting Project No. (RSP-2019/1) King Saud University, Riyadh, Saudi Arabia.

■ ABBREVIATIONS USED

CA, Carbonic Anhydrase; NHE1, sodium-hydrogen antiporter 1; AE2, Anion Exchange protein 2; NBCe1, sodium-bicarbonate cotransporter 1; MCT4, monocarboxylate transporter 4; CAI, Carbonic Anhydrase Inhibitor; SAC, Saccharin; ACE, Acesulfame K; BTD, 2H-benzo[e][1,2,4]thiadiazin-3(4H)-one-1,1-dioxide; CSI, Chlorosulfonyl Isocyanate; AAZ, Acetazolamide; VdW, Vad der Waals.

■ AUTHOR INFORMATION

*Corresponding Author:

Phone: +39-055-4573685. E-mail: alessio.nocentini@unifi.it (AN)

Phone: +39-055-4573729. Fax: +39-055-4573385. E-mail: claudiu.supuran@unifi.it (CTS)

Supporting Information

The Supporting Information is available free of charge on the ACS Publications website at DOI:

supplemental X-ray crystallographic figures and anti-proliferative assays data.

SMILES representation for compounds (CSV).

Associated content

Coordinates and structure factors for CA II in complex with **2a** (PDB: 6U4Q), **2d** (PDB: 6UGN), **2h** (PDB: 6UGR), **2i** (PDB: 6UGP), **2o** (PDB: 6UH0) and for CA IX-mimic in complex with **2a** (PDB: 6U4T), **2d** (PDB: 6UGO), **2h** (PDB: 6UGZ), and **2i** (PDB: 6UGQ) have been deposited into the PDB. Authors will release the atomic coordinates and experimental data upon article publication.

References

1. Taddei, M.L.; Giannoni, E.; Comito, G.; Chiarugi, P. Microenvironment and tumor cell plasticity: an easy way out. *Cancer Lett.* **2013**, *341*, 80–96.

2. Finger, E.C.; Giaccia, A.J. Hypoxia, inflammation, and the tumor microenvironment in metastatic disease. *Cancer Metastasis Rev.* **2010**, *29*, 285–293.

3. Neri, D.; Supuran, C.T. Interfering with pH regulation in tumours as a therapeutic strategy. *Nat. Rev. Drug. Discov.* **2011**, *10*, 767-777.

4. Nocentini, A.; Supuran, C.T. Carbonic anhydrase inhibitors as antitumor/antimetastatic agents: a patent review (2008-2018). *Expert Opin. Ther. Pat.* **2018**, *28*, 729-740.

5. Gatenby, R.A.; Smallbone, K.; Maini, P.K.; Rose, F.; Averill, J.; Nagle, R.B.; Worrall, L.; Gillies, R.J. Cellular adaptations to hypoxia and acidosis during somatic evolution of breast cancer. *Br. J. Cancer.* **2007**, *97*, 646–653.

6. Supuran, C.T. Carbonic anhydrases: novel therapeutic applications for inhibitors and activators. *Nat. Rev. Drug. Discov.* **2008**, *7*, 168-181.

7. Nocentini, A.; Supuran, C.T. Carbonic Anhydrases: An Overview. In Carbonic Anhydrases; Nocentini, A.; Supuran CT. Amsterdam: Elsevier; **2019**. p. 3-16.

8. Alterio, V.; Hilvo, M.; Di Fiore, A.; Supuran, C.T.; Pan, P.; Parkkila, S.; Scaloni, A.; Pastorek, J.; Pastorekova, S.; Pedone, C.; Scozzafava, A.; Monti, S.M.; De Simone, G. Crystal structure of the catalytic domain of the tumor-associated human carbonic anhydrase IX. *Proc. Natl. Acad. Sci. USA* **2009**, *106*, 16233–16238.

9. Whittington, D.A.; Waheed, A.; Ulmasov, B.; Shah, G.N.; Grubb, J.H.; Sly, W.S.; Christianson, D.W. Crystal structure of the dimeric extracellular domain of human carbonic anhydrase XII, a bitopic membrane protein overexpressed in certain cancer tumor cells. *Proc. Natl. Acad. Sci. USA* **2001**, *98*, 9545-9550

10. Supuran, C.T.; Alterio, V.; Di Fiore, A.; D' Ambrosio, K.; Carta, F.; Monti, S.M.; De Simone, G. Inhibition of carbonic anhydrase IX targets primary tumors, metastases, and cancer stem cells: Three for the price of one. *Med. Res. Rev.* **2018**, *38,* 1799-1836.

11. Supuran CT. How many carbonic anhydrase inhibition mechanisms exist. *J. Enzyme Inhib. Med. Chem.* **2016**; *31*; 345–360.

12. Nocentini, A.; Supuran, C.T. Advances in the structural annotation of human carbonic anhydrases and impact on future drug discovery. *Expert Opin. Drug Discov.* **2019**, *14*, 1175-1197.

13. Lomelino, C.L.; Andring, J.T.; McKenna, R. Crystallography and its impact on carbonic anhydrase research. *Int. J. Med. Chem.* **2018**, *2018*, 9419521.

14. Köhler, K.; Hillebrecht, A.; Schulze Wischeler, J.; Innocenti, A.; Heine, A.; Supuran, C.T.; Klebe, G. Saccharin inhibits carbonic anhydrases: possible explanation for its unpleasant metallic aftertaste. *Angew. Chem. Int. Ed. Engl.* **2007**, *46*, 7697-7699

15. Mahon, B.P.; Hendon, A.M.; Driscoll, J.M.; Rankin, G.M.; Poulsen, S.A.; Supuran, C.T.; McKenna, R. Saccharin: a lead compound for structure-based drug design of carbonic anhydrase IX inhibitors. *Bioorg. Med. Chem.* **2015**, *23*, 849-854.

16. Koruza, K.; Mahon, B.P.; Blakeley, M.P.; Ostermann, A.; Schrader, T.E.; McKenna. R.; Knecht, W.; Fisher, S.Z. Using neutron crystallography to elucidate the basis of selective inhibition of carbonic anhydrase by saccharin and a derivative. *J. Struct. Biol.* **2019**, *205,* 147-154.

17. Murray, A.B.; Lomelino, C.L.; Supuran, C.T.; McKenna, R. "Seriously sweet": acesulfame K exhibits selective inhibition using alternative binding modes in carbonic anhydrase isoforms. *J. Med. Chem.* **2018**, *61*, 1176-1181.

18. Carradori, S.; Secci, D.; De Monte, C.; Mollica, A.; Ceruso, M.; Akdemir, A.; Sobolev, A.P.; Codispoti, R.; De Cosmi, F.; Guglielmi, P.; Supuran CT. A novel library of saccharin and acesulfame derivatives as potent and selective inhibitors of carbonic anhydrase IX and XII isoforms. *Bioorg. Med. Chem.* **2016**, *24,* 1095-1105.

19. De Monte, C.; Carradori, S.; Secci, D.; D'Ascenzio, M.; Vullo, D.; Ceruso, M.; Supuran, C.T. Cyclic tertiary sulfamates: selective inhibition of the tumor-associated carbonic anhydrases IX and XII by N- and O-substituted acesulfame derivatives. *Eur. J. Med. Chem.* **2014**, *84*, 240-246.

20. Nocentini, A.; Vullo, D.; Bartolucci, G.; Supuran, C.T. N-Nitrosulfonamides: A new chemotype for carbonic anhydrase inhibition, *Bioorg. Med. Chem.* **2016**, *24*, 3612-3617;

21. Bozdag, M.; Alafeefy, A.M.; Altamimi, A.M.; Vullo, D.; Carta, F.; Supuran, C.T. Coumarins and other fused bicyclic heterocycles with selective tumor-associated carbonic anhydrase isoforms inhibitory activity. *Bioorg. Med. Chem.* **2017**, *25*, 677-683

22. Kornahrens, A.F.; Cognetta, A.B.; Brody, D.M.; Matthews, M.L.; Cravatt, B.F.; Boger, D.L. Design of benzoxathiazin-3-one 1,1-dioxides as a new class of irreversible serine hydrolase inhibitors: discovery of a uniquely selective PNPLA4 inhibitor. *J. Am. Chem. Soc.* **2017**, *139*, 7052-7061.

23. Zhang, S.; Chen, X.; Parveen, S.; Hussain, S.; Yang, Y.; Jing, C.; Zhu, C. Effect of C7 modifications on benzothiadiazine-1,1-dioxide derivatives on their inhibitory activity and selectivity toward aldose reductase. *ChemMedChem.* **2013**, *8*, 603-613.

24. Khalifah, R.G. The carbon dioxide hydration activity of carbonic anhydrase. *J. Biol. Chem.* **1971**, *246*, 2561−2573.

25. Nocentini, A.; Bua, S.; Lomelino, C.L.; McKenna, R.; Menicatti, M.; Bartolucci, G.; Tenci, B.; Di Cesare Mannelli, L.; Ghelardini, C.; Gratteri, P.; Supuran, C.T. Discovery of new sulfonamide carbonic anhydrase IX inhibitors incorporating nitrogenous bases. *ACS Med. Chem. Lett.* **2017**, *8*, 1314-1319.

26. Nocentini, A.; William A. Donald, Supuran CT, Human Carbonic Anhydrases: Tissue Distribution, Physiologic Role, and Druggability. In Carbonic Anhydrases; Nocentini, A.; Supuran CT. Amsterdam: Elsevier; **2019**. p. 149-185

27. Ilie, M.; Mazure, N. M.; Hofman, V.; Ammadi, R.E.; Ortholan, C.; Bonnetaud, C.; Havet, K.; Venissac, N.; Mograbi, B.; Mouroux, J.; Pouysségur, J.; Hofman, P. High levels of carbonic anhydrase IX in tumour tissue and plasma are biomarkers of poor prognostic in patients with non-small cell lung cancer. *Br. J. Cancer*. **2010**, *102*, 1627–1635.

28. Ambrosio, M.R.; Di Serio, C.; Danza, G.; Rocca, B.J., Ginori, A.; Prudovsky, I.; Marchionni, N.; Del Vecchio, M.T.; Tarantini, F. Carbonic anhydrase IX is a marker of hypoxia and correlates with higher Gleason scores and ISUP grading in prostate cancer. *Diagn. Pathol*. **2016**, *11*, p.45.

29. Korkeila, E.; Talvinen, K.; Jaakkola, P.M.; Minn, H.; Syrjänen, K.; Sundström, J.; Pyrhönen, S. Expression of carbonic anhydrase IX suggests poor outcome in rectal cancer, *Br. J. Cancer*. **2009**, *100*, 874–880.

30. Mosmann, T. Rapid colorimetric assay for cellular growth and survival: application to proliferation and cytotoxicity assays. *J. Immunol. Methods* **1983**, *65*, 55–63.

31. Coviello, V.; Marchi, B.; Sartini, S.; Quattrini, L.; Marini, A.M.; Simorini, F.; Taliani, S.; Salerno, S.; Orlandi, P.; Fioravanti, A.; Desidero, T.D. 1, 2-Benzisothiazole derivatives bearing 4-, 5-, or 6-alkyl/arylcarboxamide moieties inhibit carbonic anhydrase isoform IX (CAIX) and cell proliferation under hypoxic conditions. *J. Med. Chem*. **2016**, *59*, 6547–6552.

32. Marshall, A. G.; Hendrickson, C. L. High-resolution mass spectrometers. *Annu. Rev. Anal. Chem.* **2008**, 1, 579–599.

33. Nocentini, A.; Ceruso, M.; Bua, S.; Lomelino, C.L.; Andring, J.T.; McKenna, R.; Lanzi, C.; Sgambellone, S.; Pecori, R.; Matucci, R.; Filippi, L.; Gratteri, P.; Carta, F.; Masini, E.; Selleri, S.; Supuran, C.T. Discovery of β-adrenergic receptors blocker-carbonic anhydrase inhibitor hybrids for multitargeted antiglaucoma therapy. *J. Med. Chem.* **2018**, *61*, 5380-5394

34. Nocentini, A.; Gratteri, P.; Supuran, C.T. Phosphorus versus sulfur: discovery of benzenephosphonamidates as versatile sulfonamide-mimic chemotypes acting as carbonic anhydrase inhibitors. *Chem. Eur. J.* **2019**, *25*, 1188-1192.

35. Nocentini, A.; Trallori, E.; Singh, S.; Lomelino, C.L.; Bartolucci, G.; Di Cesare Mannelli, L.; Ghelardini, C.; McKenna, R.; Gratteri, P.; Supuran, CT. 4-Hydroxy-3-nitro-5-ureido-benzenesulfonamides selectively target the tumor-associated carbonic anhydrase isoforms IX and XII showing hypoxia-enhanced antiproliferative profiles. *J. Med. Chem.* **2018**, *61*, 10860-10874.

36. Pinard, M.A.; Boone, C.D.; Rife, B.D.; Supuran, C.T.; McKenna, R. Structural study of interaction between brinzolamide and dorzolamide inhibition of human carbonic anhydrases. *Bioorg. Med. Chem.* **2013**, *21***,** 7210–7215.

37. Kabsch, W. *XDS. Acta Cryst.* **2010**, *D66*, 125-132.

38. Winn, M.D.; Ballard, C.C.; Cowtan, K.D.; Dodson, E.J.; Emsley, P.; Evans, P.R.; Keegan, R.M.; Krissinel, E.B.; Leslie, A.G.; McCoy, A.; McNicholas, S.J.; Murshudov, G.N.; Pannu, N.S.; Potterton, E.A.; Powell, H.R.; Read, R.J.; Vagin, A.; Wilson, K.S. Overview of the CCP4 suite and current developments. *Acta. Cryst.* **2011**, *D67*, 235-242.

39. Avvaru, B.S.; Kim, C.U.; Sippel, K.H.; Gruner, S.M.; Agbandje-McKenna, M.; Silverman, D.N.; McKenna, R. A short, strong hydrogen bond in the active site of human carbonic anhydrase II. *Biochemistry (Mosc.)* **2010**, *49***,** 249–251.

40. Adams, P.D.; Afonine, P.V.; Bunkóczi, G.; Chen, V.B.; Davis, I.W.; Echols, N.; Headd, J.J.; Hung, L.W.; Kapral, G.J.; Grosse-Kunstleve, R.W.; McCoy, A.J.; Moriarty, N.W.; Oeffner, R.; Read, R.J.; Richardson, D.C.; Richardson, J.S.; Terwilliger, T.C.; Zwart, P.H. *PHENIX*: a comprehensive Python-based system for macromolecular structure solution. *Acta Crystallogr. D Biol. Crystallogr.* **2010**, *66,* 213–221.

41. Emsley, P.; Cowtan, K. *Coot*: model-building tools for molecular graphics. *Acta Crystallogr. D Biol. Crystallogr.* **2004**, *60,* 2126–2132.

42. The PyMOL Molecular Graphics System, Version 1.5.0.4 Schrödinger, LLC.

43. Almahli, H.; Hadchity, E.; Jaballah, M.Y.; Daher, R.; Ghabbour, H.A.; Kabil, M.M.; Al-Shakliah, N.S.; Eldehna, W.M. Development of novel synthesized phthalazinone-based PARP-1 inhibitors with apoptosis inducing mechanism in lung cancer *Bioorg. Chem.* **2018**, *77*, 443–456.

44. Eldehna, W.M.; Almahli, H.; Al-Ansary, G.H.; Ghabbour, H.A.; Aly, M.H.; Ismael, O.E.; Al-Dhfyan, A.; Abdel-Aziz, H.A. Synthesis and in vitro anti-proliferative activity of some novel isatins

conjugated with quinazoline/phthalazine hydrazines against triple-negative breast cancer MDA-MB-231 cells as apoptosis-inducing agents. *J. Enzym. Inhib. Med. Chem.* **2017**, *32*, 600–613.

Table of Contents Graphic